electromagnetic cascades and intergalactic magnetic fields

Rafael Alves Batista

Department of Physics - Astrophysics
University of Oxford

rafael.alvesbatista@physics.ox.ac.uk

Pisa
20/10/2016

outline

- modelling the propagation of gamma rays in the universe
- intergalactic magnetic fields: origin, limits, and gamma-ray signatures
- new 3D simulation code for gamma-ray propagation: GRPropa
- simulating blazar pair haloes
- probing the magnetic helicity of intergalactic magnetic fields

modelling the propagation of gamma rays

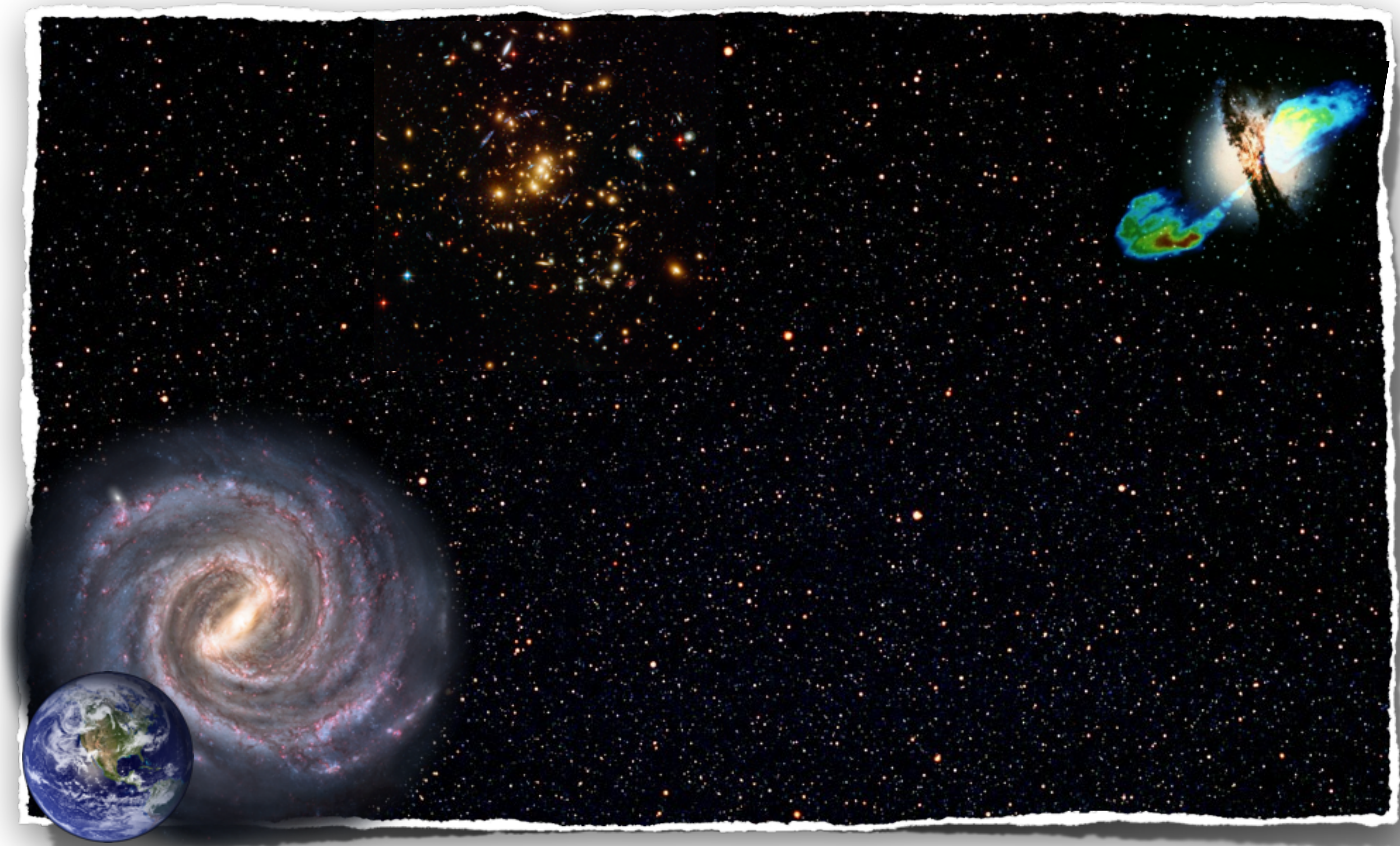

modelling the propagation of gamma rays

modelling the propagation of gamma rays

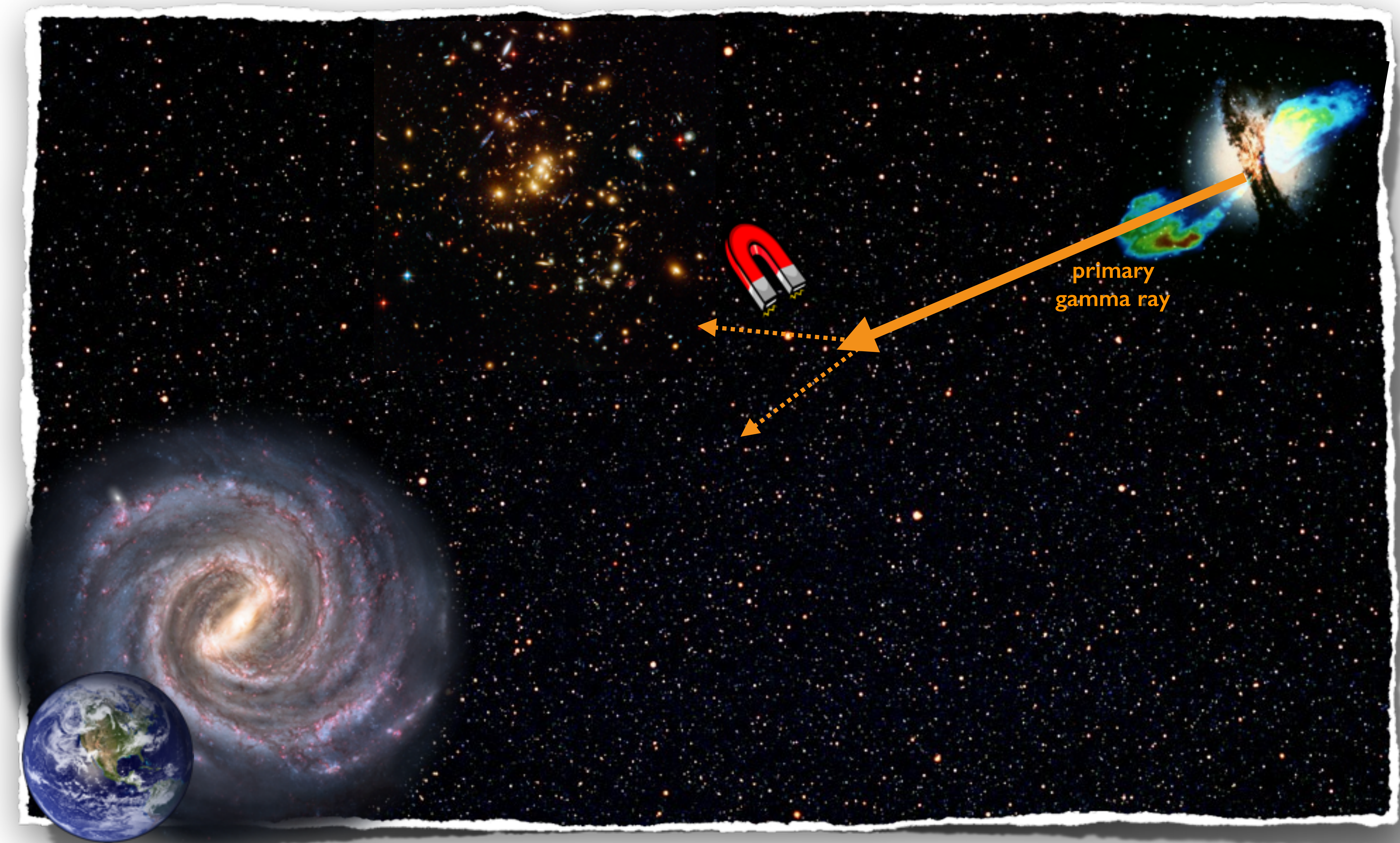

modelling the propagation of gamma rays

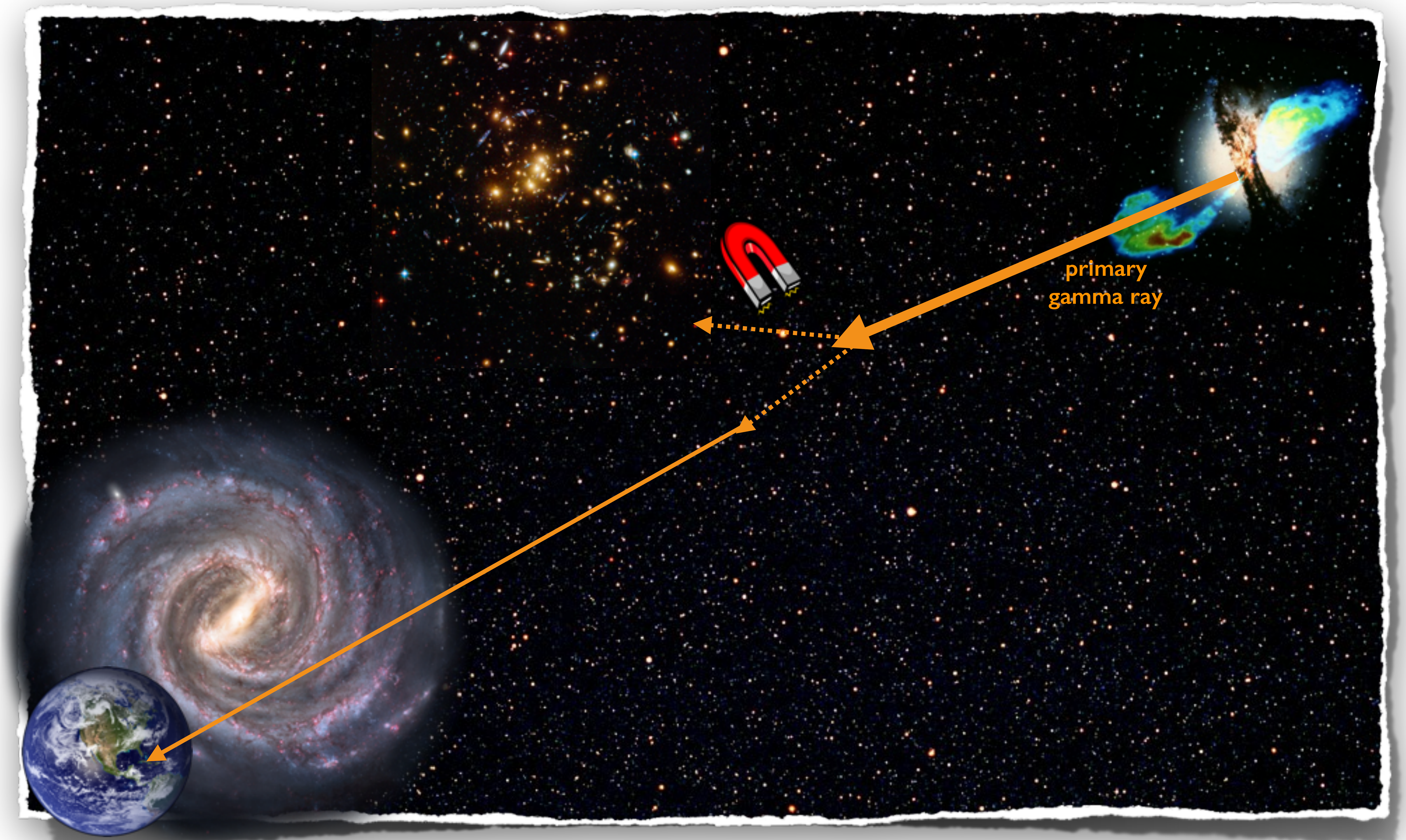

modelling the propagation of gamma rays

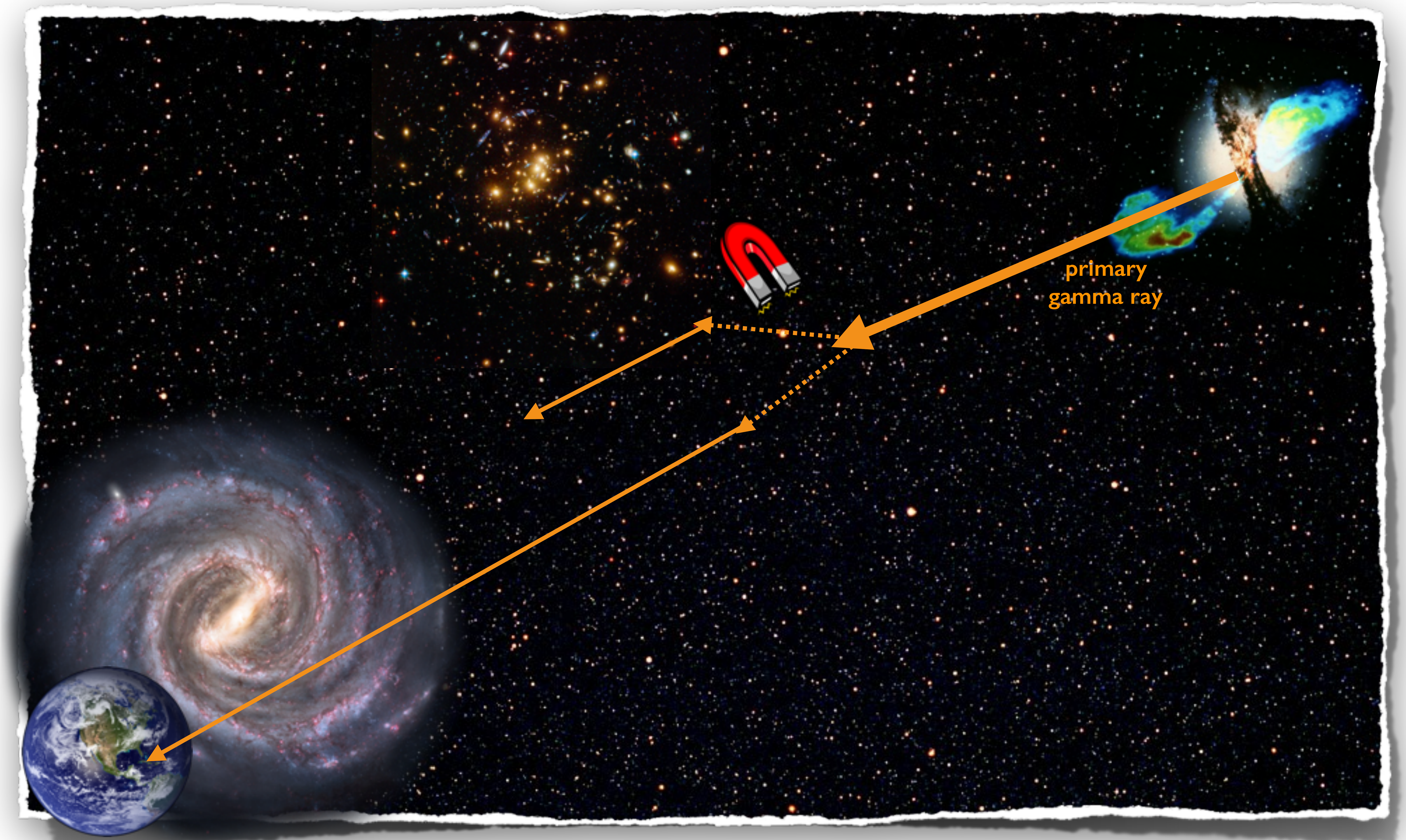

modelling the propagation of gamma rays

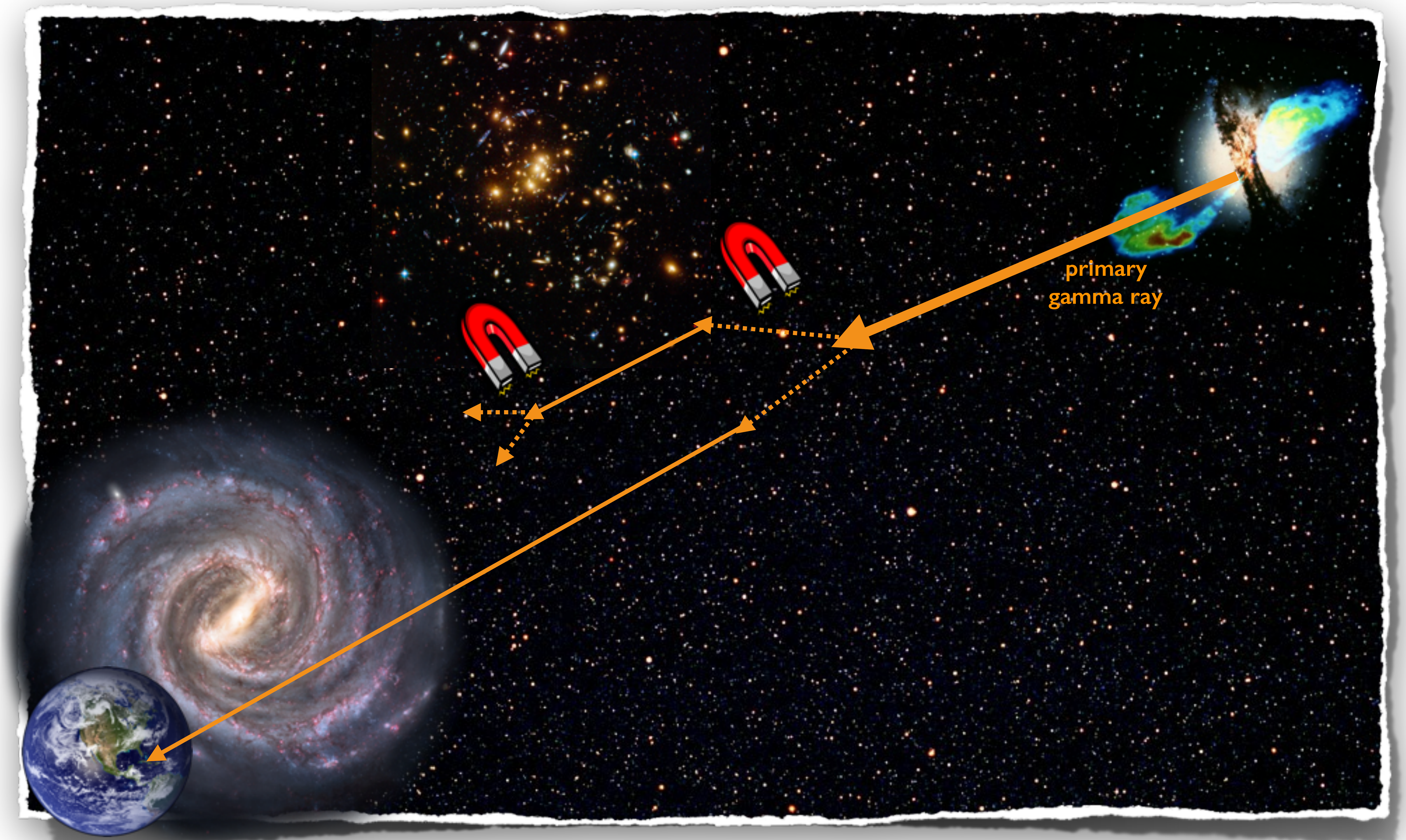

modelling the propagation of gamma rays

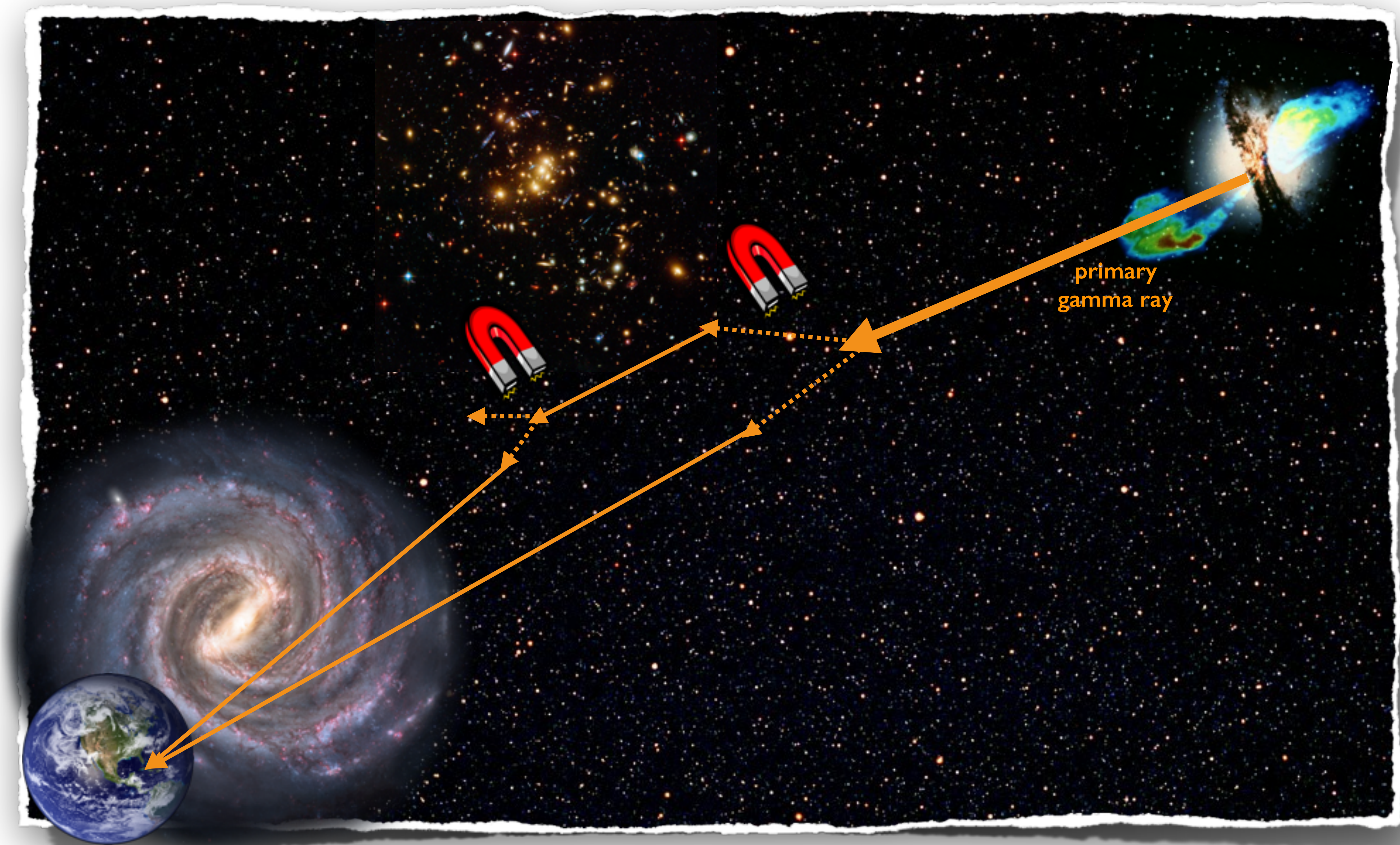

modelling the propagation of gamma rays

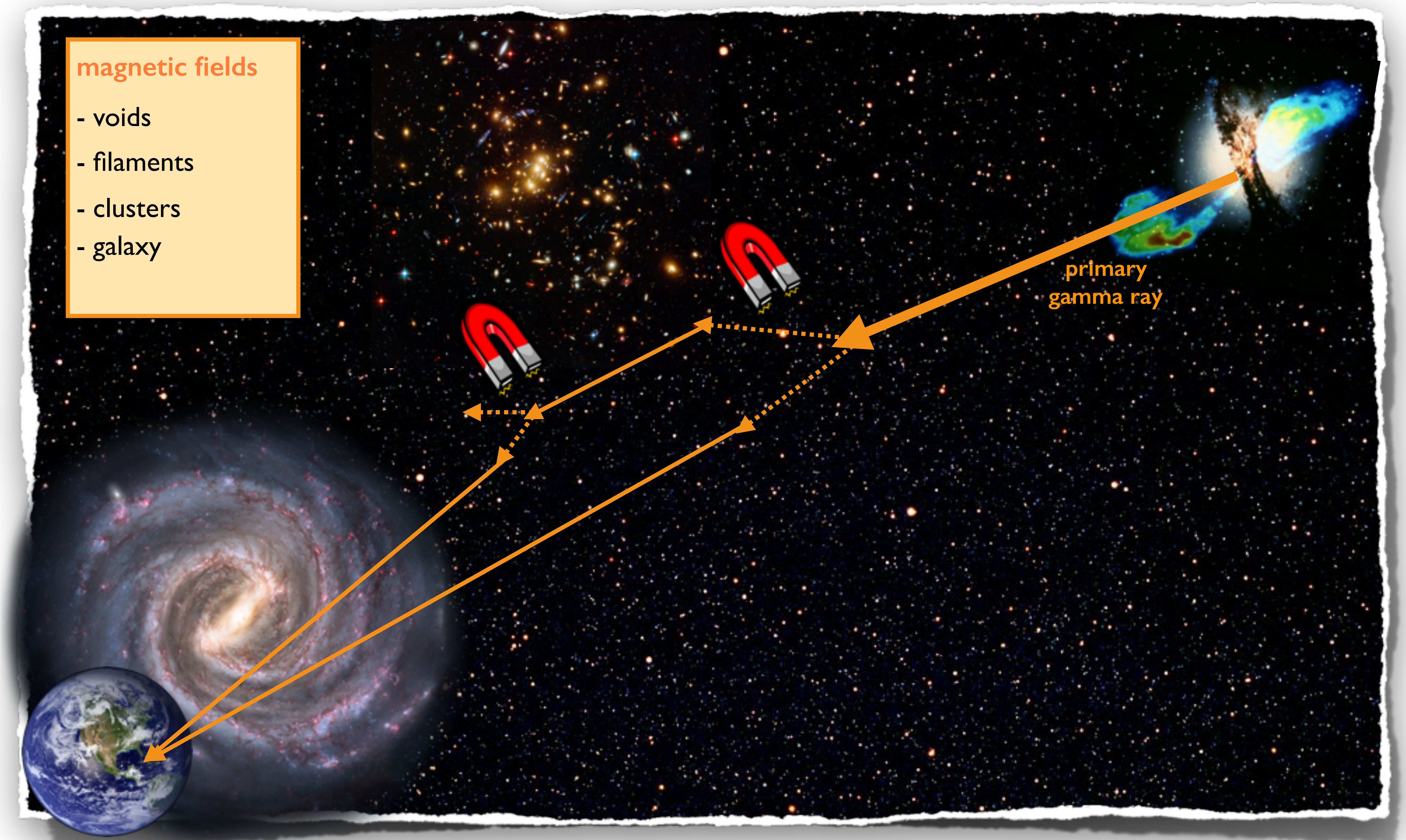

modelling the propagation of gamma rays

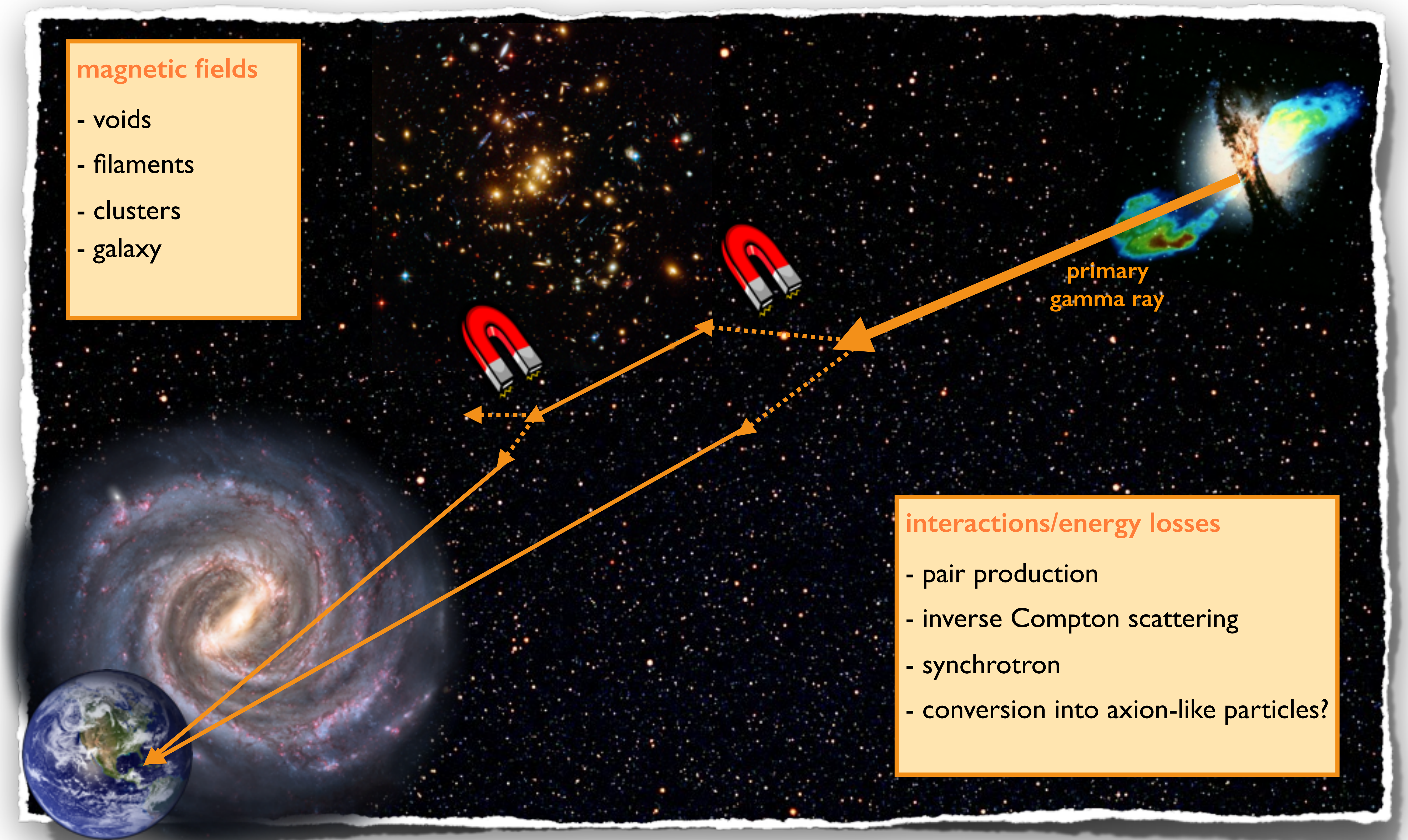

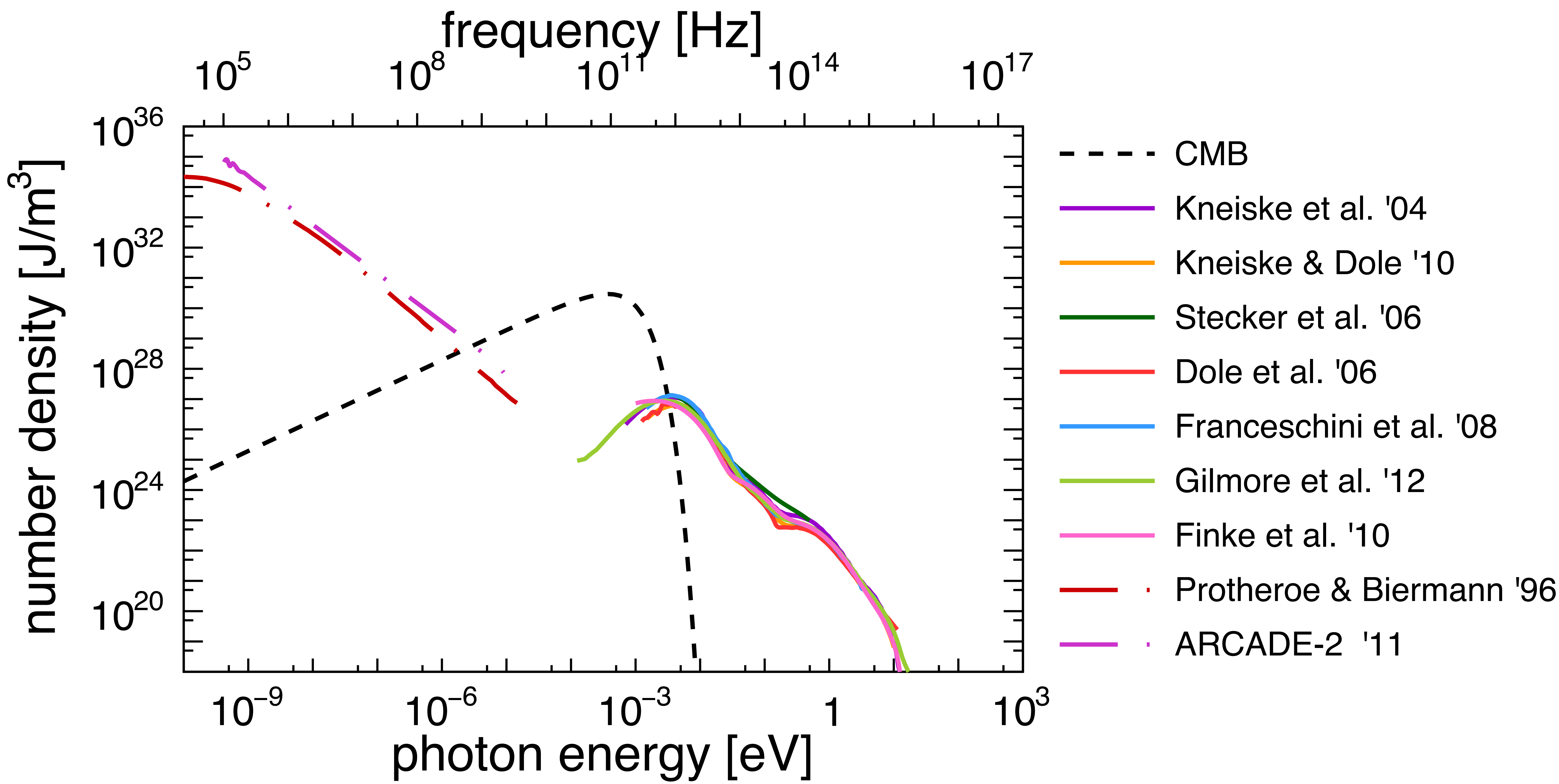
frequency [Hz]
10^5
10^8
10^11
10^14
10^17
number density [J/m^3]
10^36
10^32
10^28
10^24
10^20
10^−9
10^−6
10^−3
1
10^3
photon energy [eV]
CMB
Kneiske et al. '04
Kneiske & Dole '10
Stecker et al. '06
Dole et al. '06
Franceschini et al. '08
Gilmore et al. '12
Finke et al. '10
Protheroe & Biermann '96
ARCADE-2 '11

intergalactic magnetic fields

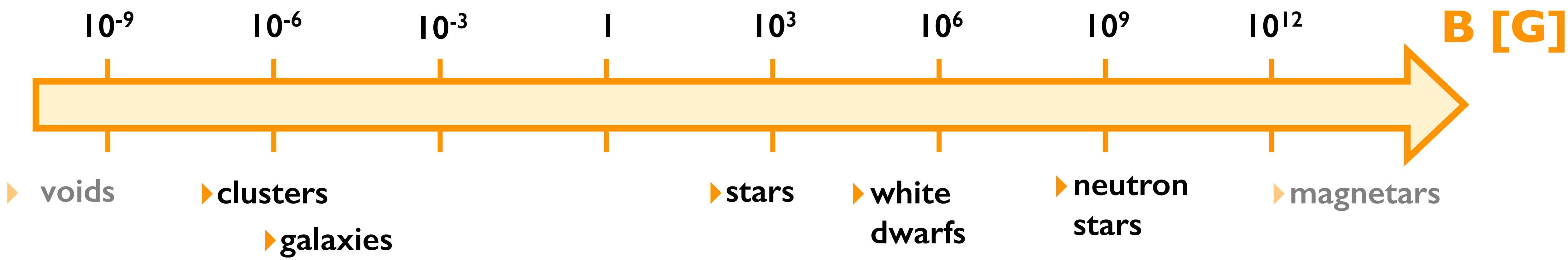

- are there cosmological magnetic fields?
- how did the magnetic fields in the universe come to be? astrophysical vs cosmological origin
- we have upper and lower bounds, but parameter space is still large
- upper limit from CMB: ~nG
  [Planck Collaboration. A&A 594 (2016) A19]
- lower limit from cascades: ~10 aG
  [Neronov & Vovk. Science 328 (2010) 72]

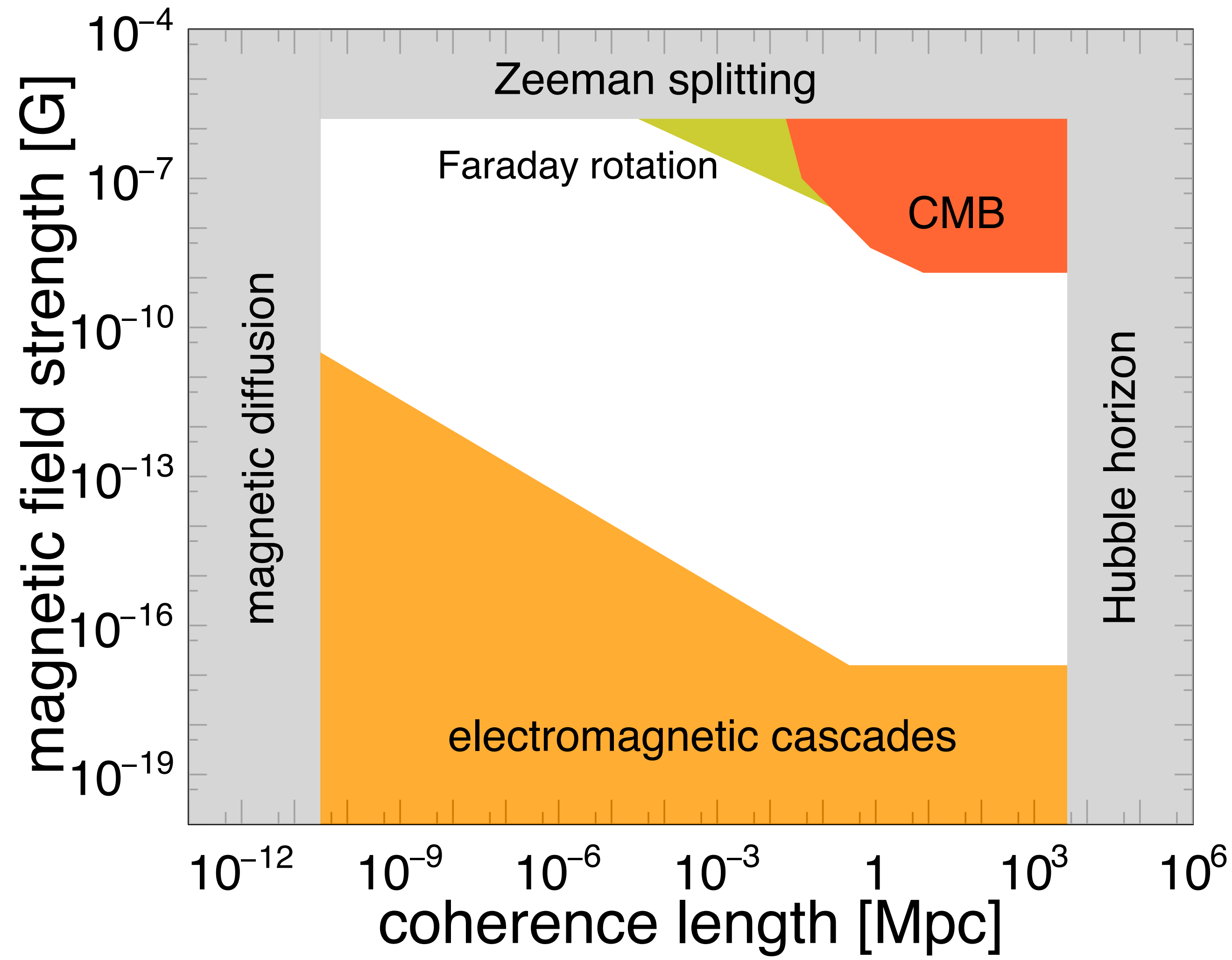

electromagnetic cascades

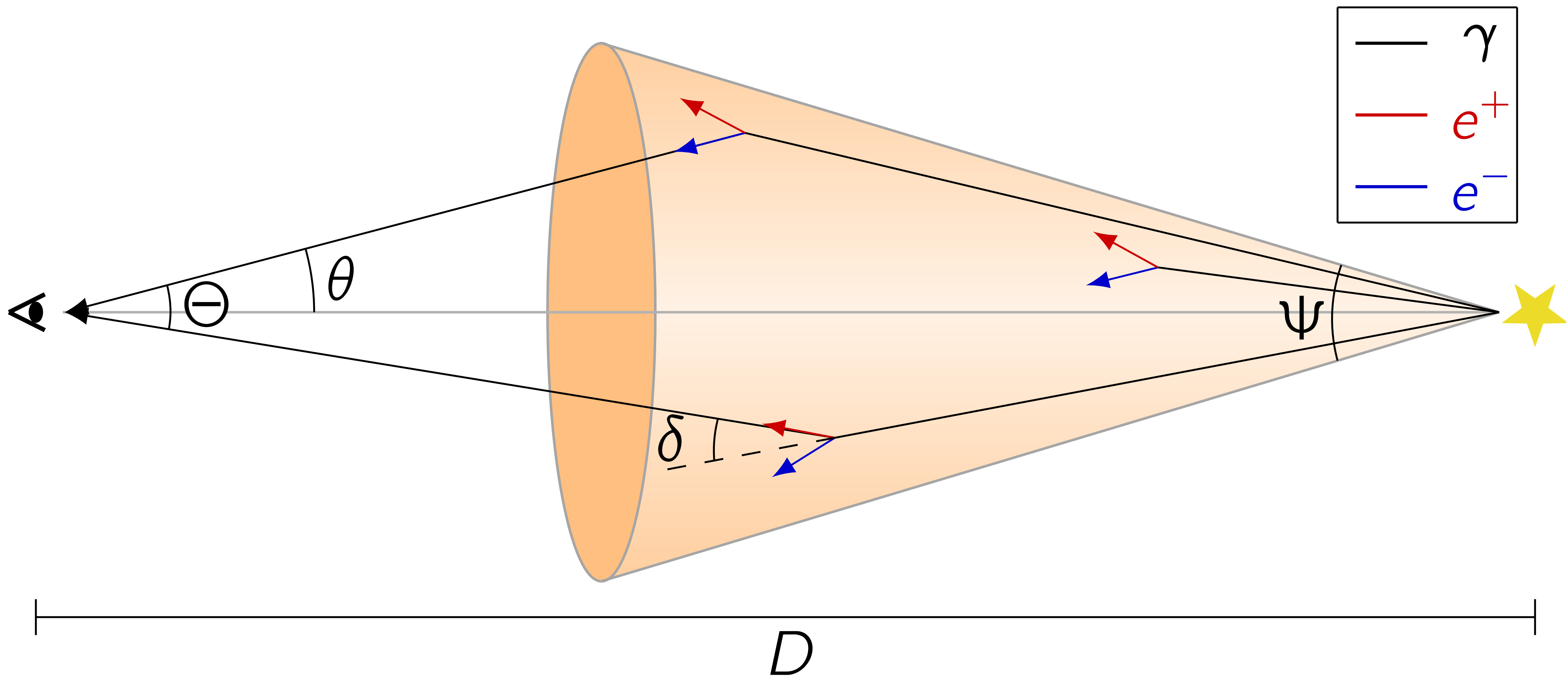

- point-like sources will appear extended
  [R. Plaga. Nature. 374 (1995) 430]
- the charged component of the cascade is sensitive to the **strength** and **structure** of intervening magnetic fields

effects of magnetic fields on the spectrum

Savelliev et al. arXiv:1311.6752

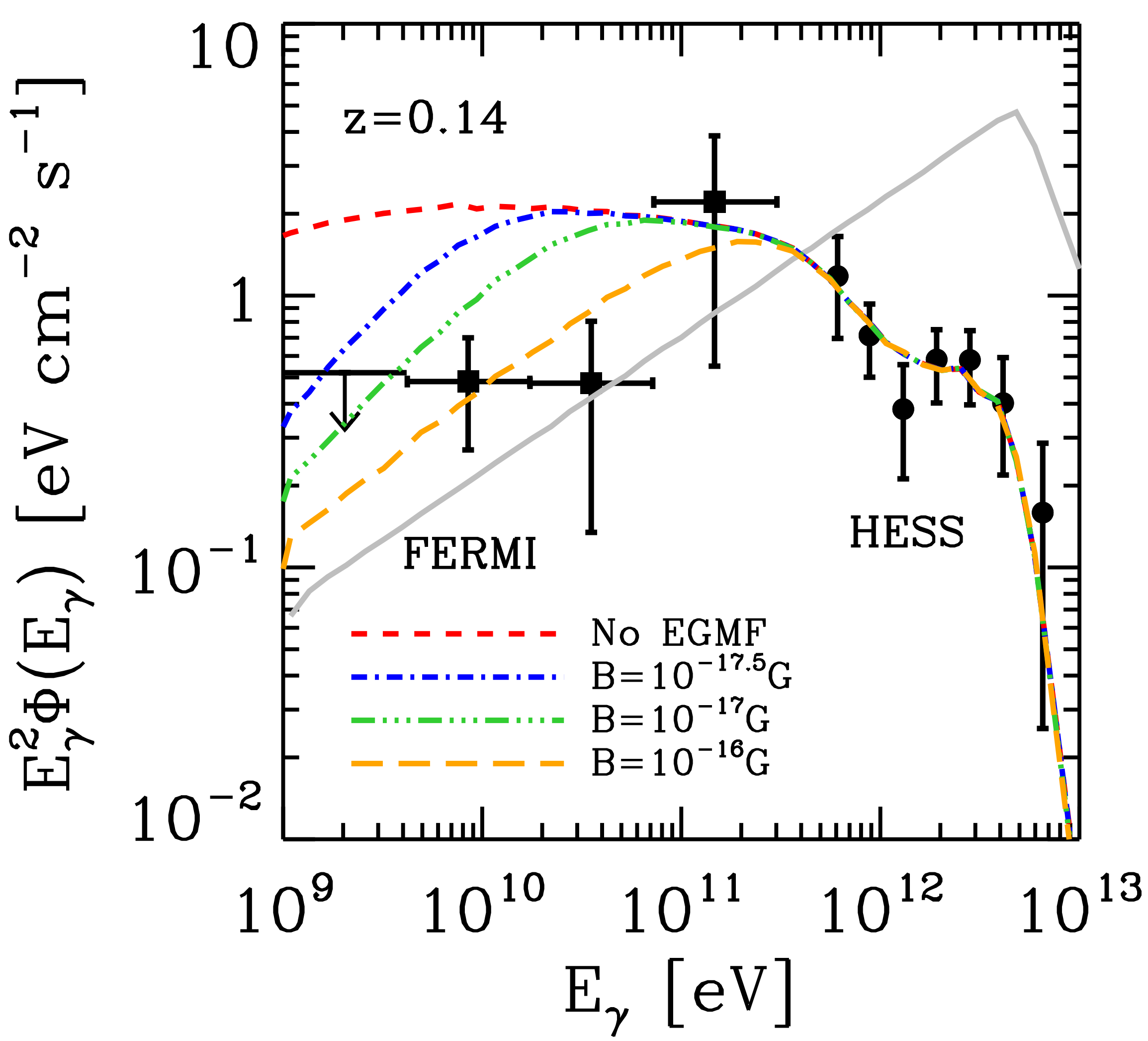

alternative explanations

- B>10^{-17} G disperses the GeV cascade
  [A. Neronov, I. Vovk. Science 328 (2010) 72; A. Taylor et al. A&A 529 (2011) A144]
- plasma instabilities suppresses the development of the cascades
  [A. Broderick et al. ApJ 752 (2012) 22; R. Schlickeiser et al. ApJ 777 (2013) 49]
- primary CRs continuously produces TeV gamma rays
  [W. Essey et al. ApJ 731 (2011) 51; W. Essey et al. PRL 104 (2010) 141102]
- gamma ray mixing with ALPs or hidden photons
  [D. Horns et al. PRD 86 (2011) 075024; M. Meyer et al. PRD 87 (2013) 035027; A. Dobrynina et al. PRD 91 (2015) 083003]
- Lorentz invariance violation
  [U. Jacob, T. Piran. PRD 78 (2008) 124010; F. Tavecchio, G. Bonnoli. A&A 585 (2016) A25]

GRPropa

- Based on the modular code structure of the CRPropa 3 code for cosmic-ray propagation
  CRPropa: github.com/CRPropa/CRPropa3 *[RAB et al. JCAP 05 (2016) 038. arXiv:1603.07142]*
- four-dimensional (3D + time) simulation of gamma-ray propagation
- other codes: Elmag (1D + time; small-angle approximation)
  [M. Kachelriess et al. Comp. Phys. Comm. 183 (2011) 1036]
- energy range: 0.1 GeV - 1 PeV (will be extended)
- "thinning" to optimise performance
- arbitrary magnetic field configurations and a few default options
- code already used in arXiv:1607.00320
  [RAB et al. Phys. Rev. D 94 (2016) 083005]

RAB, A. Saveliev. In preparation.

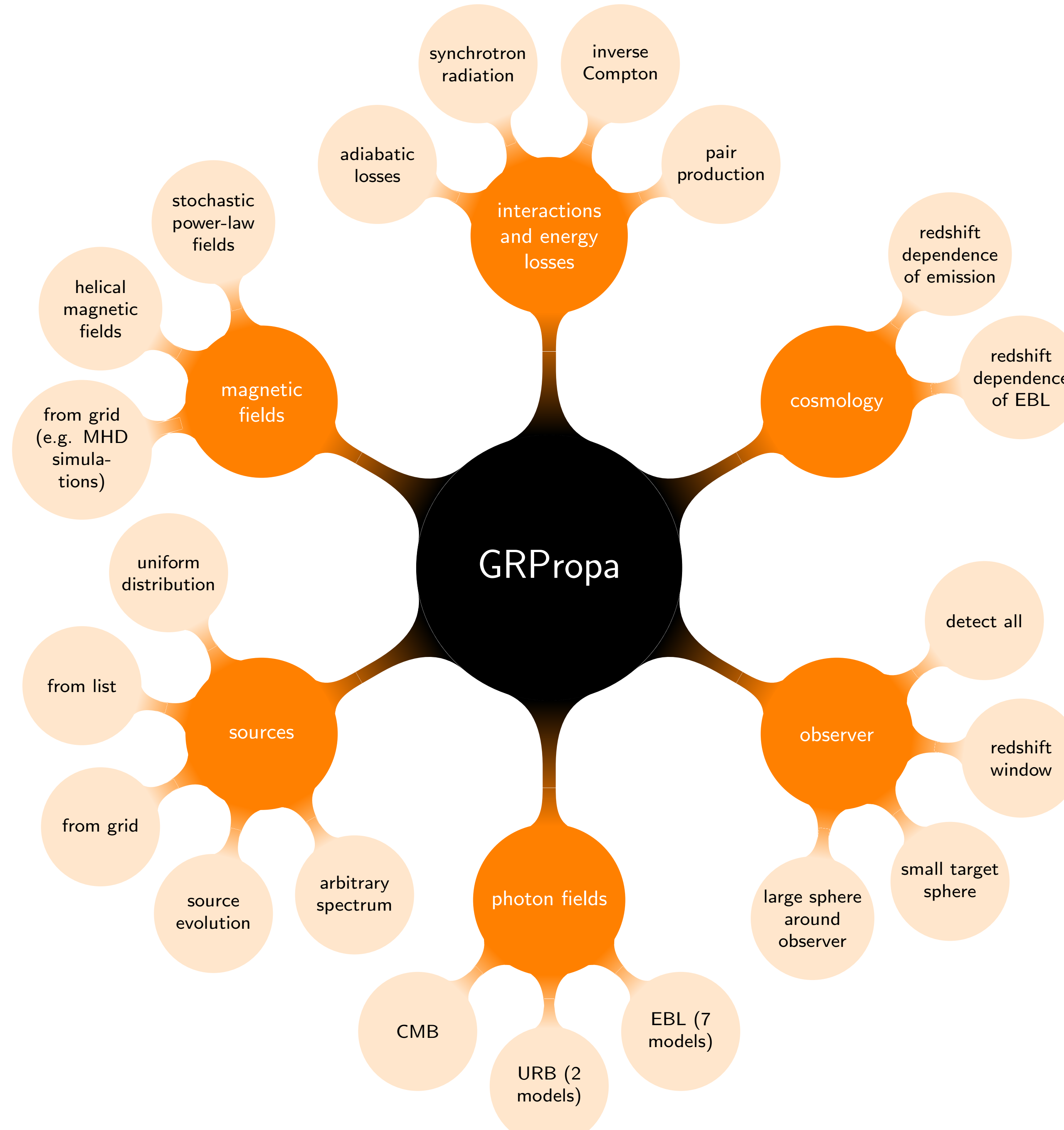

GRPropa: interactions

RAB, A. Saveliev. In preparation.

inverse Compton

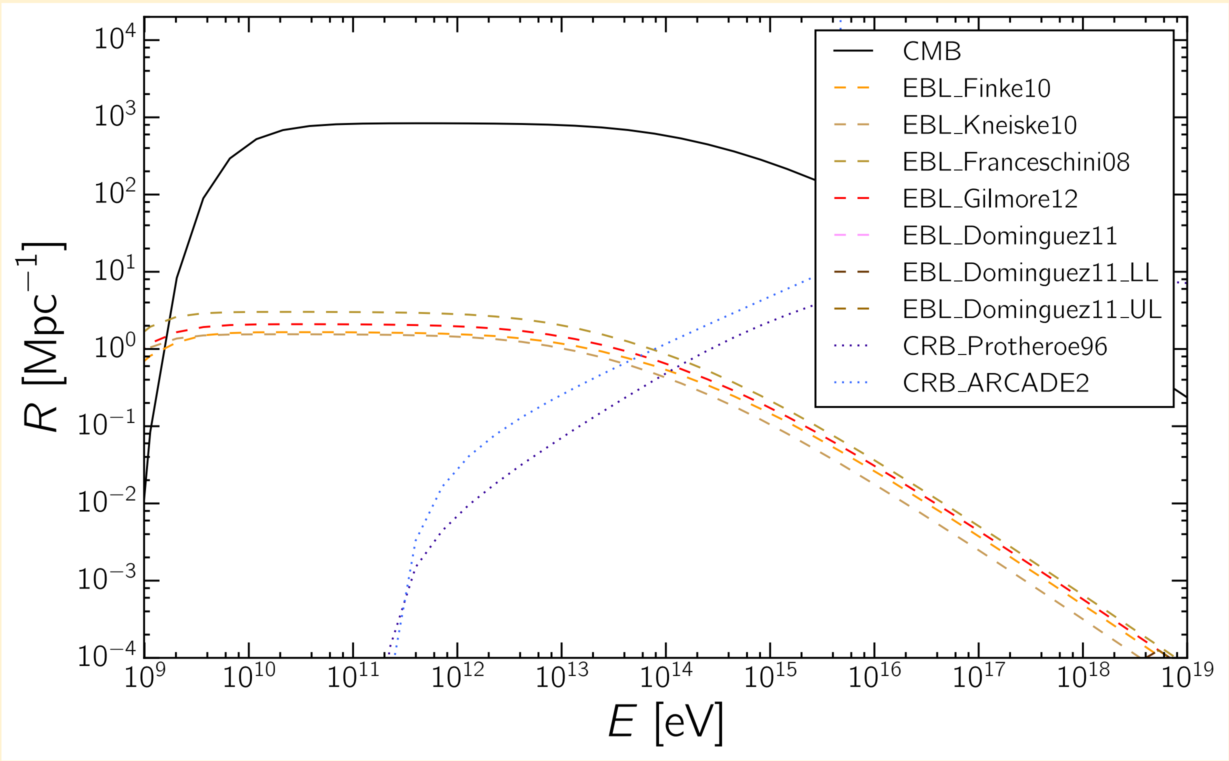

pair production

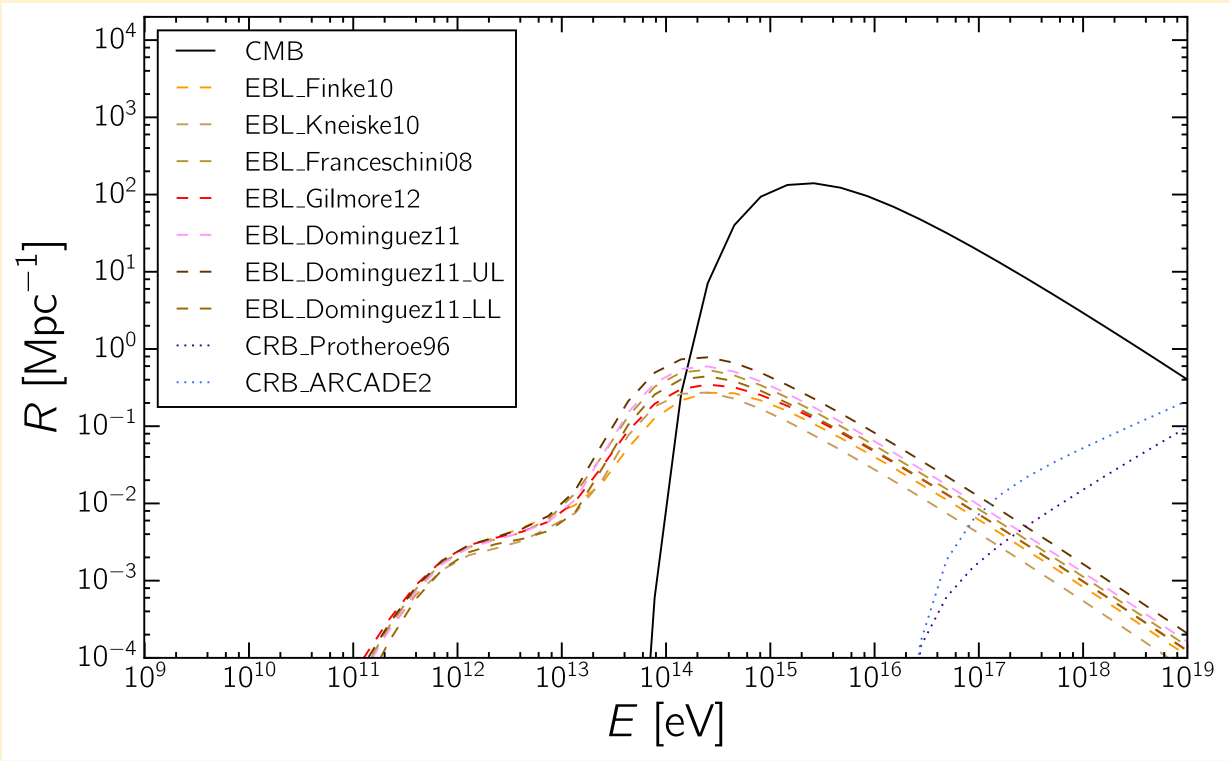

synchrotron

$$\frac{dE}{dx} \approx \frac{m_e^2 c^4 \chi^2}{\hbar c \left(1 + 4.8(1+\chi)\ln(1+1.7\chi) + 3.44\chi^2\right)^{\frac{2}{3}}} \qquad \chi = \frac{\left|\vec{p} \times \vec{B}\right|}{m_e c\, 4.4 \times 10^{13}\ \mathrm{G}}$$

redshift losses

$$\frac{dt}{dz} = \frac{1}{H_0(1+z)} \frac{1}{\sqrt{\Omega_m (1+z)^3 + \Omega_\Lambda}}$$

GRPropa: simulation of blazar pair halo

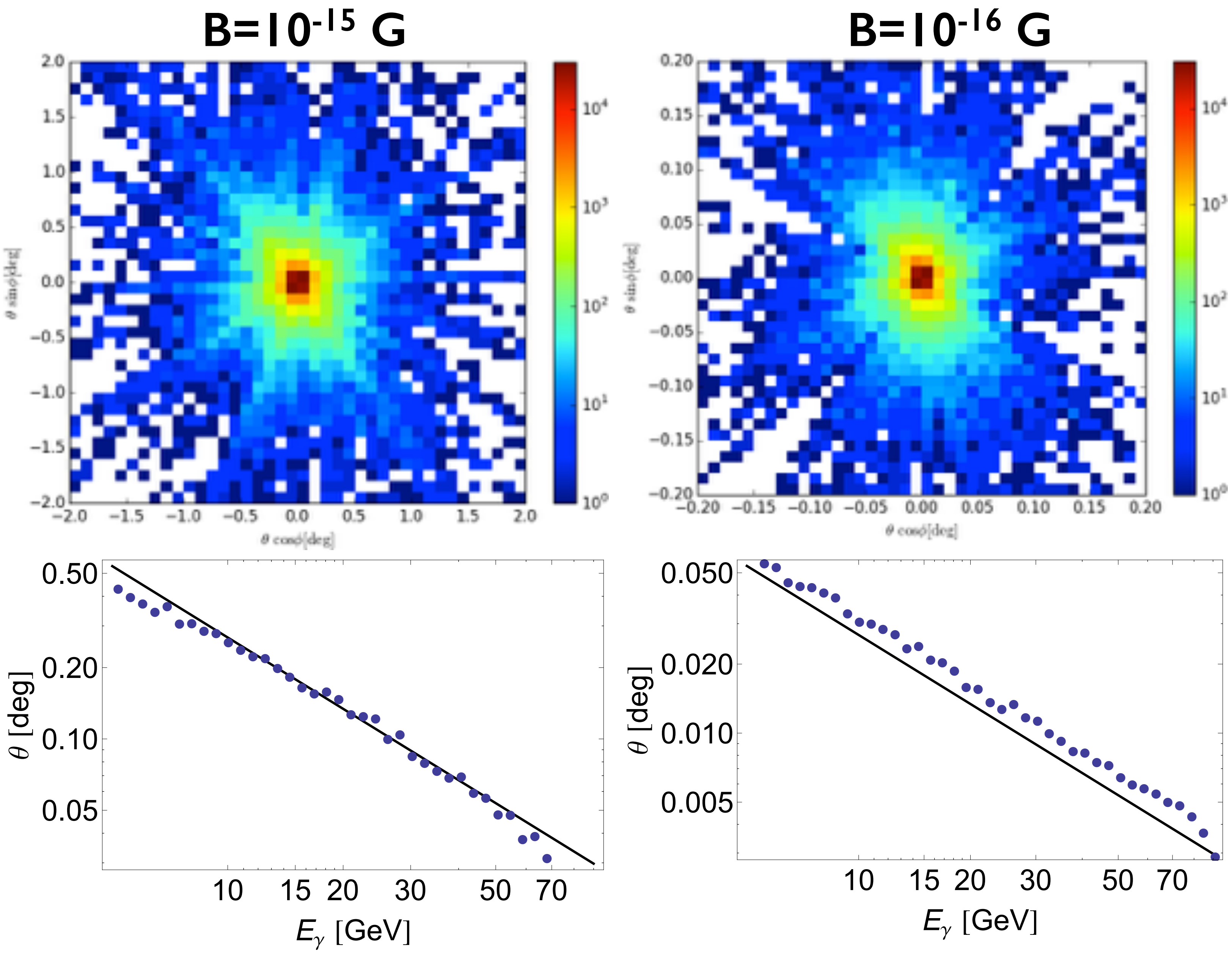

RAB, A. Saveliev, G. Sigl, T. Vachaspati. PRD 94 (2016) 083005. arXiv:1607.00320

- stochastic magnetic field with Batcherlor spectrum
- blazar located at D=1 Gpc
- performance: 10^5 initial photons , without thinning, take about 8 hours on 64 cores at 2.3 GHz

theoretical prediction

Neronov & Semikoz. PRD 80 (2009) 123012.

$$\theta(E_\gamma) \simeq 0.05^\circ \kappa (1+z_s)^{-4} \left(\frac{B}{\mathrm{fG}}\right) \left(\frac{E_\gamma}{0.1\,\mathrm{TeV}}\right)^{-1} \left(\frac{D_s}{\mathrm{Gpc}}\right)^{-1} \left(\frac{E_{\mathrm{TeV}}}{10\,\mathrm{TeV}}\right)^{-1}$$

helical intergalactic magnetic fields

- helicity $\mathcal{H} = \frac{1}{V} \int_V d^3r \, \vec{A} \cdot \vec{B}$
- helical magnetic fields may be related to baryogenesis via bubble collisions and linked Z-string creation [J. M. Cornwall PRD 56 (1996) 6146; T. Vachaspati PRL 87 (2001) 251302]
- advantage of helical magnetic fields: from MHD, we know they are less likely to dissipate
- helicity is odd under CP transformation
- parity-odd correlators give B~10 fG *[H. Tashiro & T. Vachaspati. MNRAS 448 (2015) 299]*
- morphology of arrival directions of gamma-rays can be used to infer the helicity of IGMFs *[A. Long & T. Vachaspati. JCAP 09 (2015) 065]*

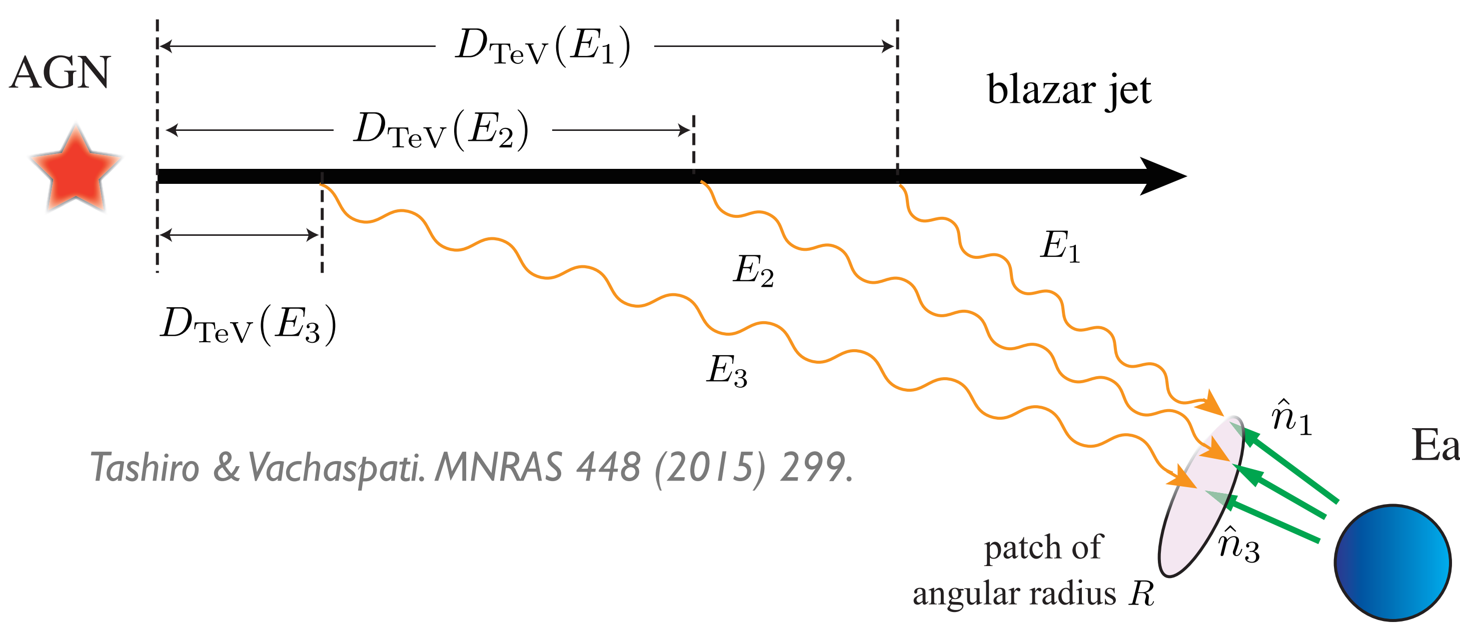

Tashiro & Vachaspati. MNRAS 448 (2015) 299.

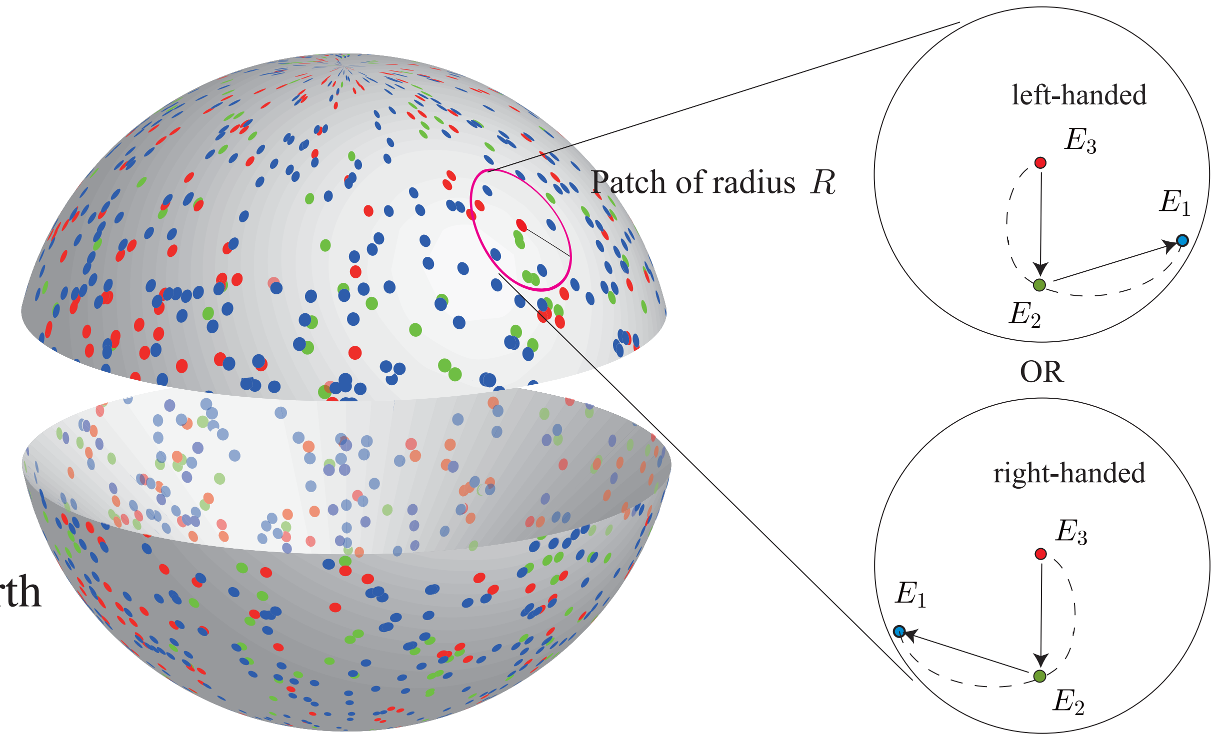

Chen et al. MNRAS Lett. 445 (2014) L41.

the S-statistics

RAB, A. Saveliev, G. Sigl, T. Vachaspati. PRD 94 (2016) 083005. arXiv:1607.00320

1. calculate average deflection per energy bin

$$\bar{\theta}(\phi^{(j)}, E_\gamma) = \frac{1}{N_j} \sum_{\{i|\phi^{(j)} \leq \phi_i < \phi^{(j+1)}\}} \theta_i$$

2. estimate Φ_+ and Φ_-

$$\Phi_- = \sum_{j=j_{\max}-\delta_{\text{bin}}}^{j_{\max}-1} \bar{\theta}(\phi^{(j)}, E_\gamma) \quad \Phi_+ = \sum_{j=j_{\max}+1}^{j_{\max}+\delta_{\text{bin}}} \bar{\theta}(\phi^{(j)}, E_\gamma)$$

3. compute S

$$S = \frac{\Phi_- - \Phi_+}{\Phi_- + \Phi_+}$$

δ_{bin}: number of bins necessary to fully encompass the peak

(φ_i, θ_i): coordinates of the i-th event in the bin

- S<0 for a left-handed spiral, and S>0 if the spiral is right-handed
- alternative method: Q-statistics

  [H. Tashiro et al. MNRAS Lett. 445 (2014) L41; H. Tashiro & T. Vachaspati. MNRAS 448 (2015) 299;]

S-statistics: application

RAB, A. Saveliev, G. Sigl, T. Vachaspati. PRD 94 (2016) 083005.
arXiv:1607.00320

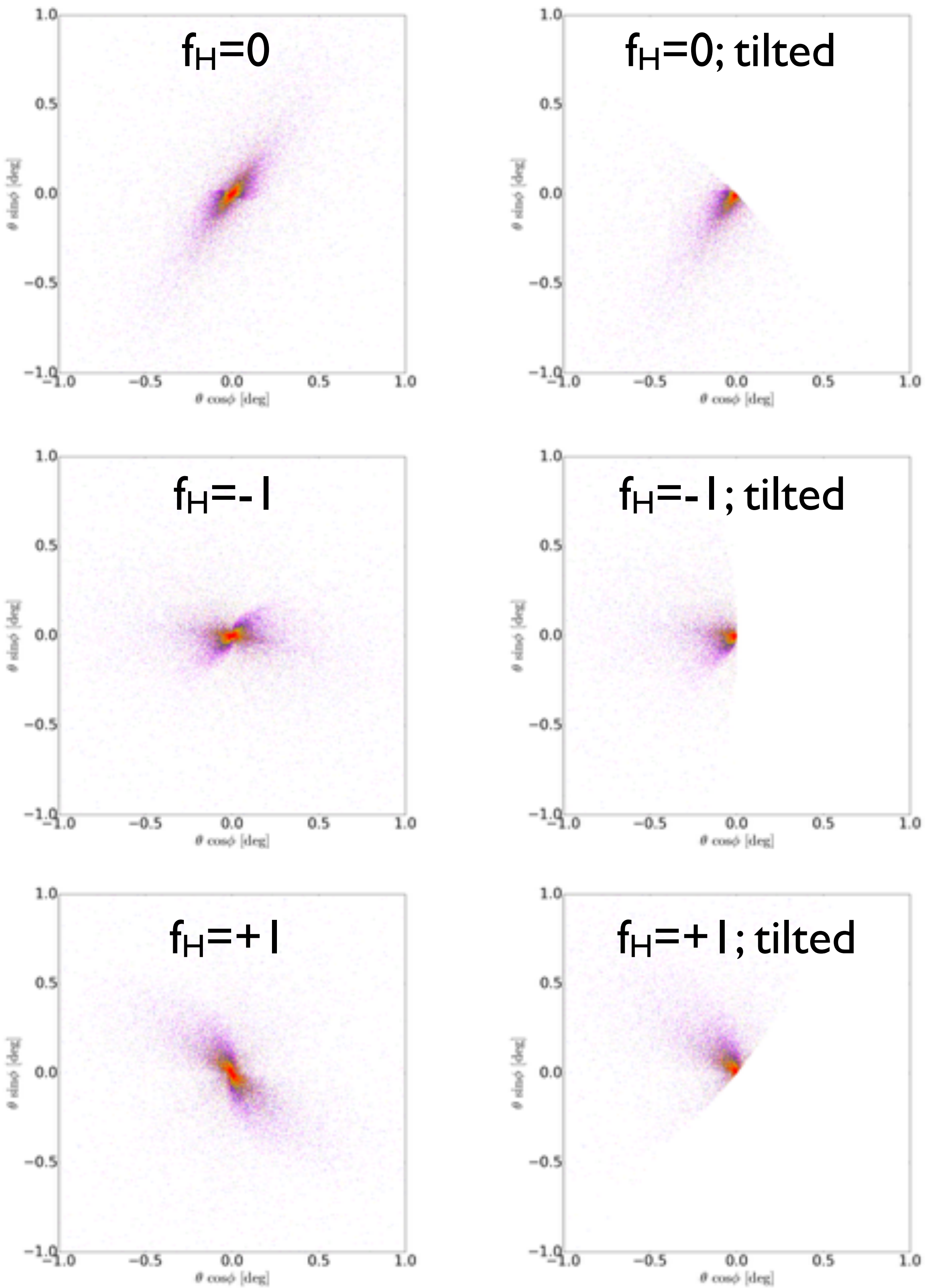

magenta: E=5-10 GeV
blue: E=10-15 GeV
green: E=15-20 GeV
yellow: E=20-30 GeV
orange: E=30-50 GeV
red: E=50-100 GeV

E_γ/GeV	j_{max}	ϕ_{max}/deg	Φ_-	Φ_+	S
5–10	6	108.0	0.768	1.67	-0.37
	16	288.0	0.649	1.60	-0.42
10–15	7	126.0	0.813	0.904	-0.05
	17	306.0	0.709	0.882	-0.11
15–20	7	126.0	0.472	0.818	-0.27
	18	324.0	0.637	0.473	0.15
20–30	6	108.0	0.222	0.625	-0.48
	17	306.0	0.370	0.428	-0.07
30–50	6	108.0	0.163	0.507	-0.51
	16	288.0	0.170	0.385	-0.39
50–100	7	126.0	0.151	0.200	-0.13
	17	306.0	0.145	0.172	-0.09

E_γ/GeV	j_{max}	ϕ_{max}/deg	Φ_-	Φ_+	S
5–10	19	342.0	1.23	1.01	+0.10
	9	162.0	1.15	1.32	-0.07
10–15	19	342.0	0.888	0.713	+0.11
	9	162.0	0.785	0.822	-0.02
15–20	0	0.0	0.722	0.284	+0.44
	9	162.0	0.594	0.542	+0.05
20–30	19	342.0	0.428	0.309	+0.16
	10	180.0	0.655	0.405	+0.24
30–50	19	342.0	0.296	0.203	+0.19
	9	162.0	0.285	0.338	-0.08
50–100	19	342.0	0.157	0.131	+0.09
	10	180.0	0.120	0.138	+0.18

Batchelor spectrum
tilt angle: 5°
D=1 Gpc
B=1 fG
Ψ=5°

S-statistics: application

RAB, A. Saveliev, G. Sigl, T. Vachaspati. PRD 94 (2016) 083005.
arXiv:1607.00320

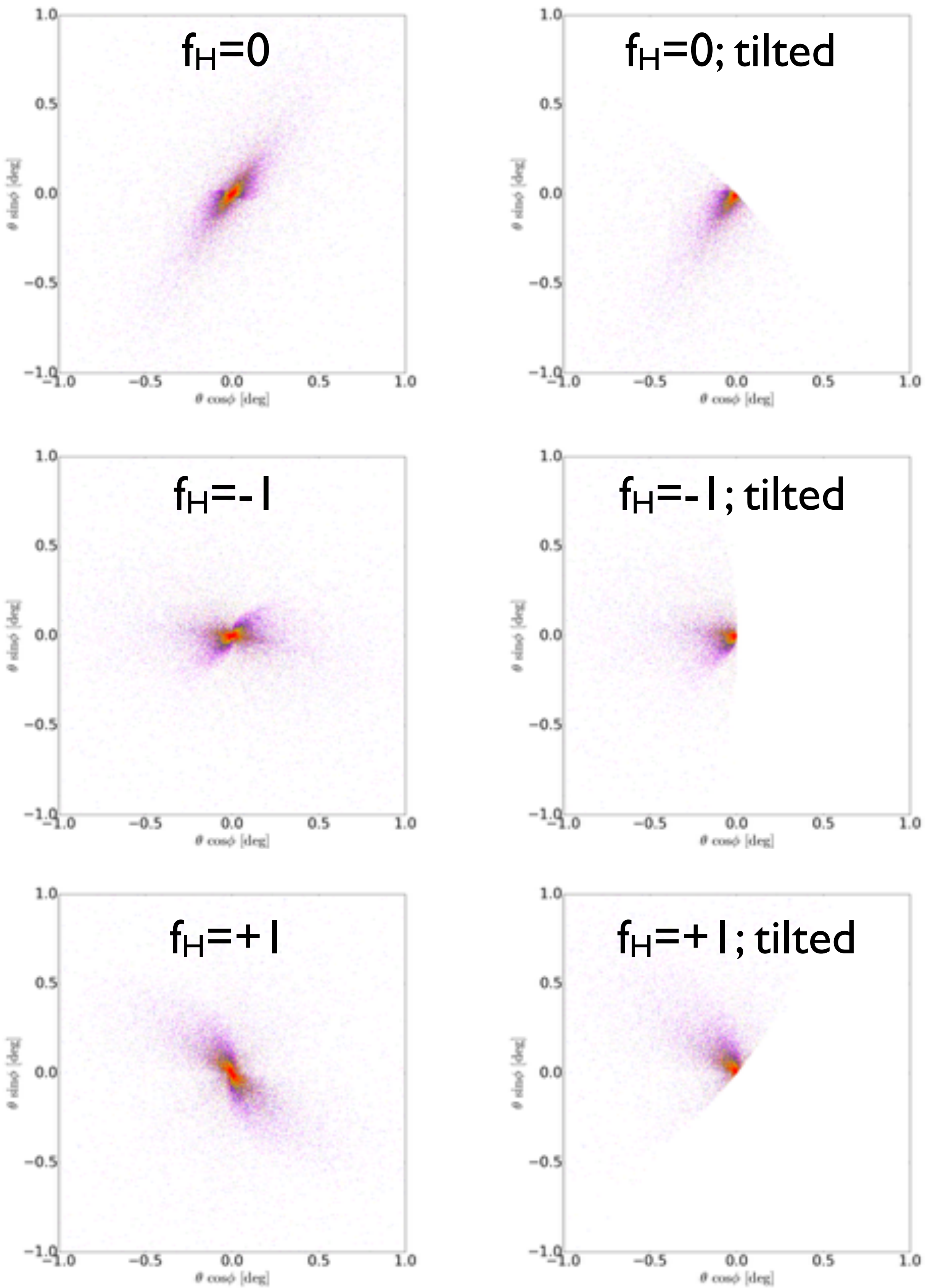

magenta: E=5-10 GeV
blue: E=10-15 GeV
green: E=15-20 GeV
yellow: E=20-30 GeV
orange: E=30-50 GeV
red: E=50-100 GeV

Batchelor spectrum
tilt angle: 5°
D=1 Gpc
B=1 fG
Ψ=5°

E_γ/GeV	j_{max}	ϕ_{max}/deg	Φ_-	Φ_+	S
5–10	6	108.0	0.768	1.67	-0.37
	16	288.0	0.649	1.60	-0.42
10–15	7	126.0	0.813	0.904	-0.05
	17	306.0	0.709	0.882	-0.11
15–20	7	126.0	0.472	0.818	-0.27
	18	324.0	0.637	0.473	0.15
20–30	6	108.0	0.222	0.625	-0.48
	17	306.0	0.370	0.428	-0.07
30–50	6	108.0	0.163	0.507	-0.51
	16	288.0	0.170	0.385	-0.39
50–100	7	126.0	0.151	0.200	-0.13
	17	306.0	0.145	0.172	-0.09

E_γ/GeV	j_{max}	ϕ_{max}/deg	Φ_-	Φ_+	S
5–10	19	342.0	1.23	1.01	+0.10
	9	162.0	1.15	1.32	-0.07
10–15	19	342.0	0.888	0.713	+0.11
	9	162.0	0.785	0.822	-0.02
15–20	0	0.0	0.722	0.284	+0.44
	9	162.0	0.594	0.542	+0.05
20–30	19	342.0	0.428	0.309	+0.16
	10	180.0	0.655	0.405	+0.24
30–50	19	342.0	0.296	0.203	+0.19
	9	162.0	0.285	0.338	-0.08
50–100	19	342.0	0.157	0.131	+0.09
	10	180.0	0.120	0.138	+0.18

RAB, A. Saveliev, G. Sigl, T. Vachaspati. PRD 94 (2016) 083005.
arXiv:1607.00320

the effect of the coherence length

for maximally positive helicity

Lc = 50 Mpc

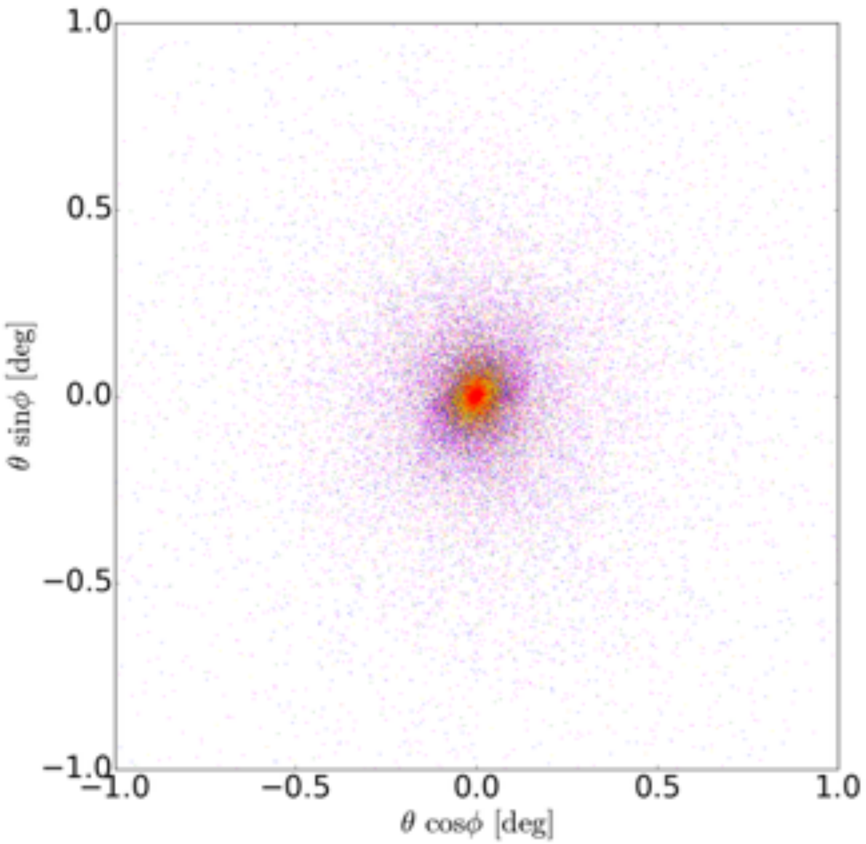

Lc = 150 Mpc

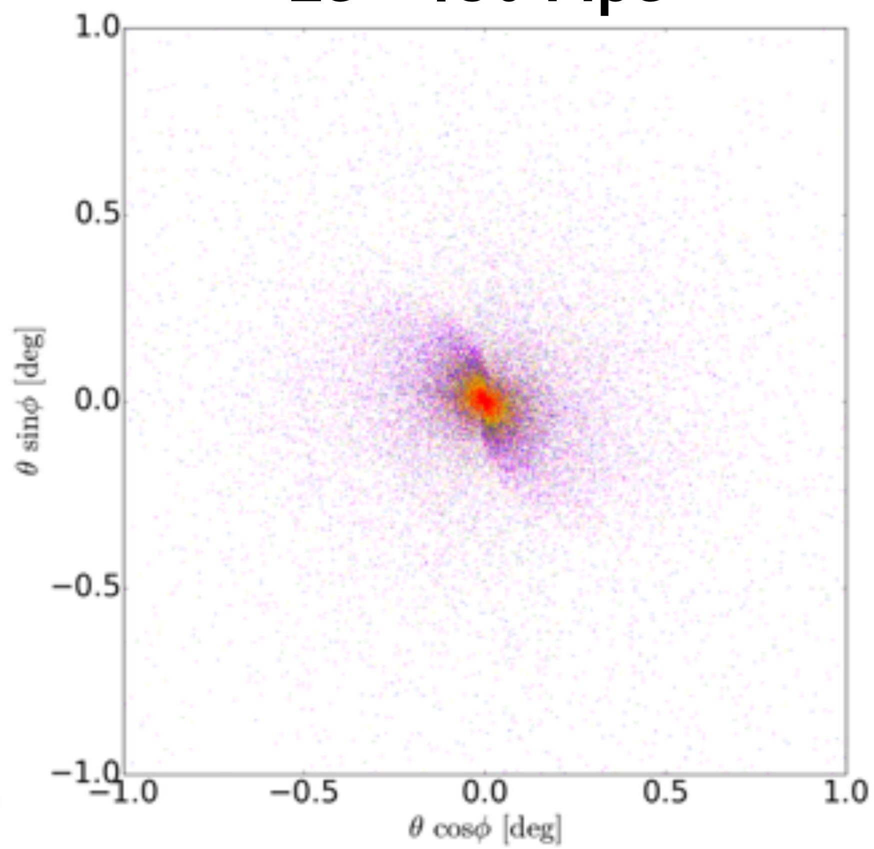

Lc = 250 Mpc

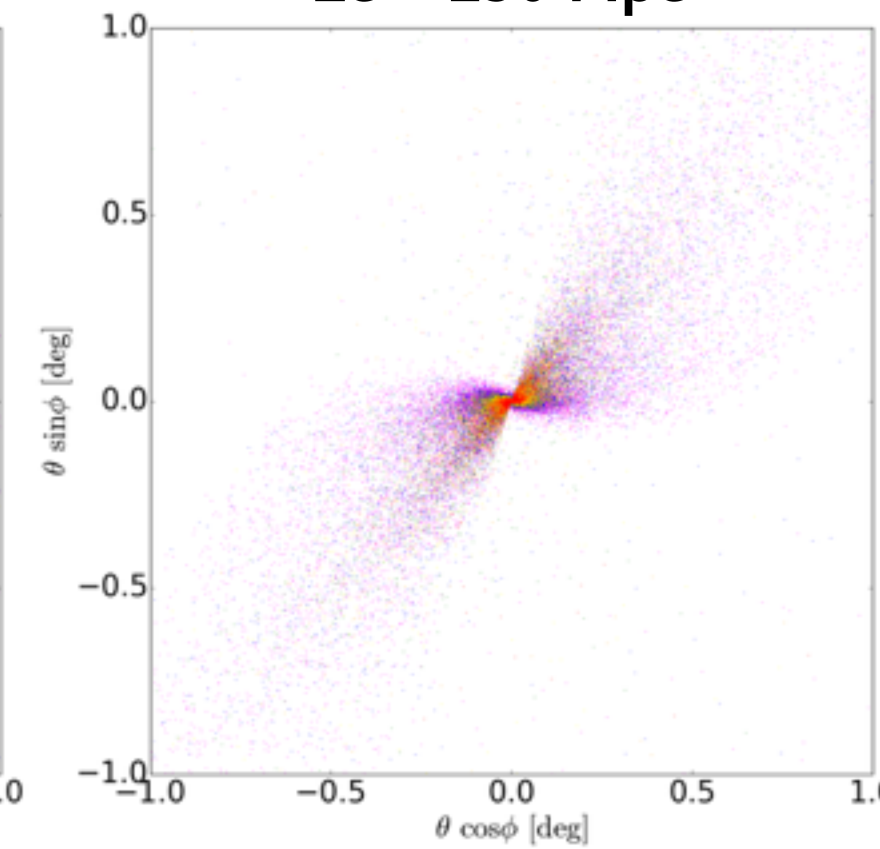

helical intergalactic magnetic fields

RAB, A. Saveliev, G. Sigl, T. Vachaspati. PRD 94 (2016) 083005.
arXiv:1607.00320

the effect of the coherence length

for maximally positive helicity

Lc = 50 Mpc **Lc = 150 Mpc** **Lc = 250 Mpc**

conclusions and outlook

- GRPropa: 3D code for propagation of electromagnetic cascades; it is up and running; further testing is still required.
- lower bound on intergalactic magnetic fields from cascades favours a primordial origin, providing us with a direct window to the early universe
- the S-statistics has been successfully tested in simulated datasets and can satisfactorily detect signatures of helicity in gamma-ray data
- observations of blazar pair haloes allow measurements of intergalactic magnetic fields, both its strength and its structure

conclusions and outlook

- GRPropa: 3D code for propagation of electromagnetic cascades; it is up and running; further testing is still required.
- lower bound on intergalactic magnetic fields from cascades favours a primordial origin, providing us with a direct window to the early universe
- the S-statistics has been successfully tested in simulated datasets and can satisfactorily detect signatures of helicity in gamma-ray data
- observations of blazar pair haloes allow measurements of intergalactic magnetic fields, both its strength and its structure

thank you :-)

Backup slides

comparison GRPropa-Elmag

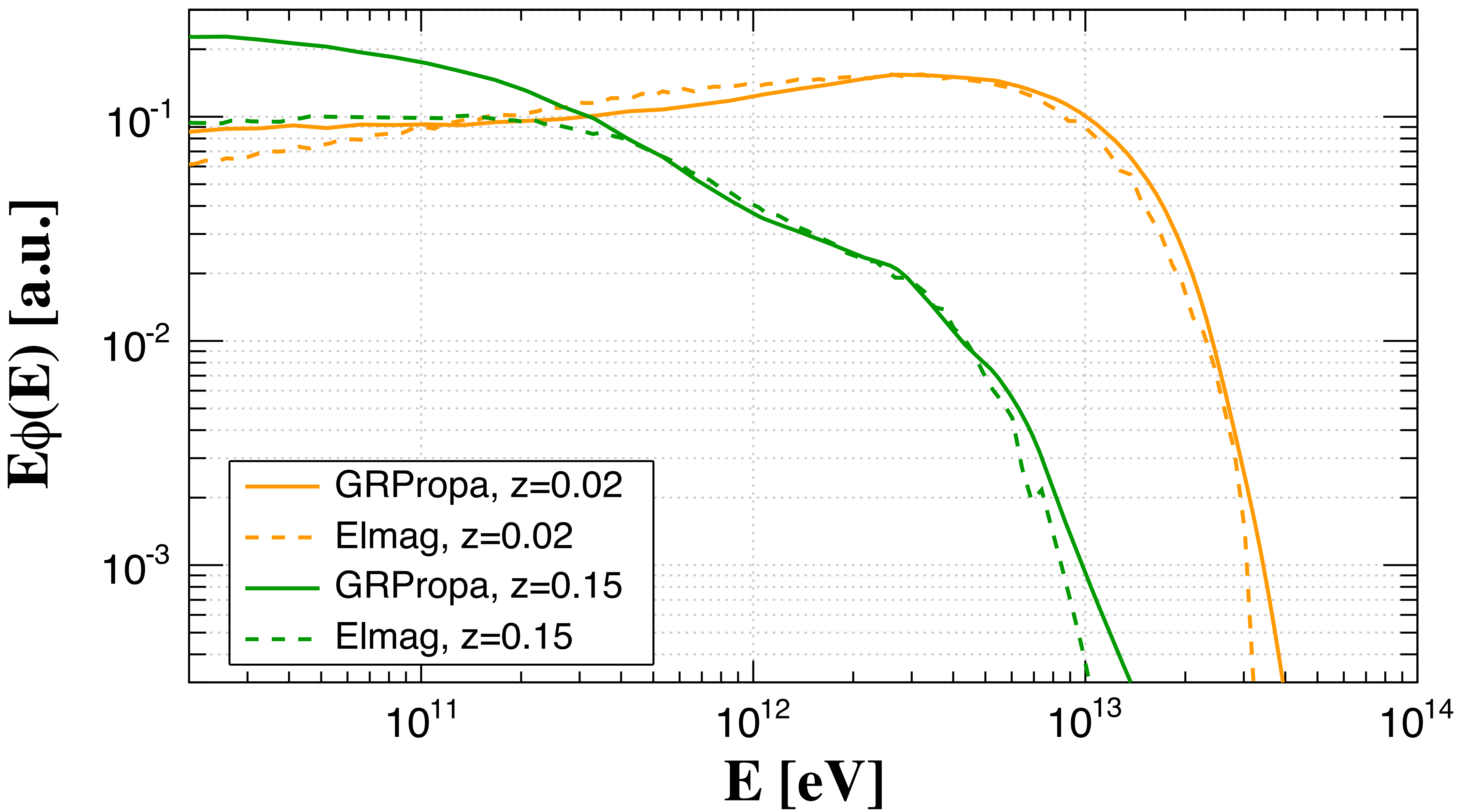

sampling helical fields: tests

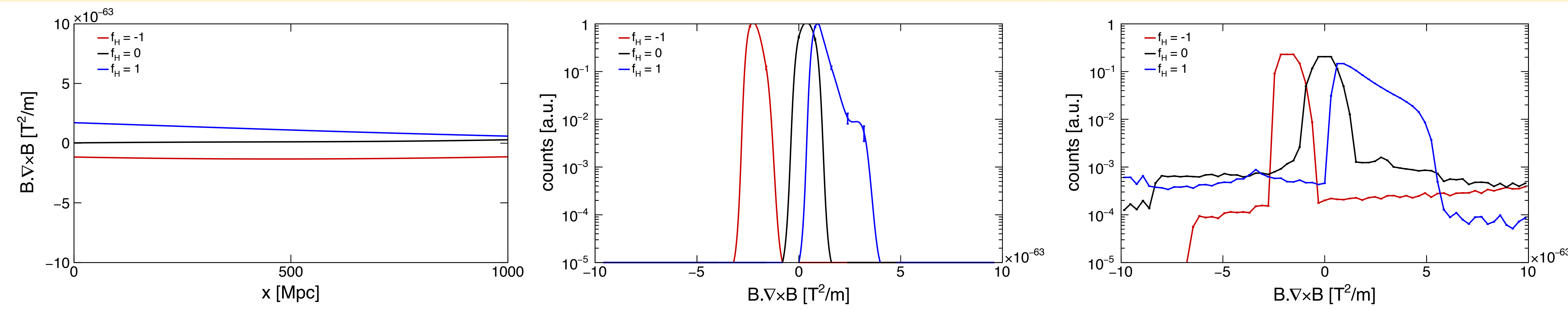

helicity-baryogenesis connection

- in electroweak baryogenesis models, in order to generate baryons, the Chern-Simons number has to change
- bubble collisions induce the creation of entities such as sphalerons, whose decay induces baryon number violation and generates magnetic helicity

Chern-Simons number

$$CS = \frac{N_f}{32\pi^2} \int d^3x \epsilon_{ijk} \left[g^2 W^a_{ij} W^{ak} - \frac{g^3}{3} W^{ai} W^{bj} W^{ck} - g^2 g'^2 Y^{ij} Y^k \right]$$

N_f: number of particle families

W^{xa}: SU(2) hypercharge gauge field

Y^x: U(1) hypercharge gauge field

g: SU(2) gauge coupling

g': U(1) gauge coupling

EW magnetogenesis - EW baryogenesis connection

$$\partial_\mu j^\mu_{B+L} = 2N_f \left(\frac{g^2}{32\pi^2} W\tilde{W} - \frac{g'^2}{32\pi^2} Y\tilde{Y} \right)$$

$$\Delta N_{B+L} = 2N_f \left(\Delta N_{CS} - \frac{\alpha_Y}{4\pi} \Delta H_Y \right)$$